Abacus, Pages 210-230, Vol.18, No.2, 1989

# COMPUTATION OF CHEMICALLY REACTING UNSTEADY ONE-DIMENSIONAL FLOWS

J.A. Olorunmaiye**
Department of Mechanical Engineering
The University of Calgary, Calgary, Alberta T2N 1N4
CANADA.

## ABSTRACT

A mathematical model of one-dimensional chemically reacting flow is presented. The effects of wall friction, heat transfer and gradual area change are included in addition to the effects of chemical reaction on the composition and specific heats of the gas. The set of quasi-linear hyperbolic partial differential equations obtained are solved by a numerical method of characteristics. The equations for various boundary conditions are also presented.

The model was applied to a shock tube in which no chemical reaction took place. The pressure at the closed left end of the shock tube predicted with the model was in very good agreement with the result obtained by Rudinger using a graphical method of characteristics.

The model was also applied to a simple quarter-wavelength organ-pipe pulsed combustor. The combustion process was modelled using a simple overall reaction rate equation. The model predicted pressure amplitudes that are in good qualitative agreement with experimental results.

** Present address: Department of Mechanical Engineering, University of Ilorin, Ilorin, Nigeria.

## 1. INTRODUCTION

Unsteady chemically reacting one-dimensional flows occur in pulsed combustors, exhaust system of internal combustion engines, shock tubes and propulsive nozzles. If the fuel-air ratio is small, the assumption of simple heating in which no notice is given to the changes in chemical composition, molecular weight and specific heats may be made. But in some cases, negligence of chemical reaction effects on composition and specific heats may yield inaccurate results. For instance, Cline [1] in his three-dimensional steady flow analysis of a rocket propulsive nozzle reported that the predicted thrust may differ between frozen and equilibrium flow by as much as 15%.

In their mathematical model, Clarke and Craigen [2] treated the combustion process in a simple organ-pipe pulsed combustor as heat addition to air. They had to use an unrealistically high gas emissivity to obtain reasonable temperature in the combustor. The work reported in this paper is an extension of their work to include the effect of chemical reaction on composition and specific heats in modelling unsteady one-dimensional flows such as occur in pulsed combustors.

## 2. MATHEMATICAL MODEL

Assuming the flow to be one-dimensional and neglecting molecular diffusion, longitudinal viscous and conductive effects, the conservation equations for mass, momentum, energy and species are

$$\frac{1}{\rho}\frac{D\rho}{Dt} + \frac{\partial u}{\partial x} + \frac{u}{a}\frac{da}{dx} = 0 \qquad (1)$$

$$\frac{Du}{Dt} + \frac{1}{\rho}\frac{\partial p}{\partial x} + w = 0 \qquad (2)$$

$$\frac{Dh}{Dt} - \frac{1}{\rho}\frac{Dp}{Dt} = q + uw \qquad (3)$$

$$\frac{DC_i}{Dt} = R_i \qquad (4)$$

where $\rho$ is the density, t is time, u is the velocity, x is the space coordinate, a is the cross-sectional area, p is the pressure, w is the frictional force per unit mass, h is the enthalpy, q is the heat transfer rate to the fluid per unit mass, and $C_i$ is the mass fraction of the i-th species.

The chemical source function for each of the N species,

$$g_i = g_i(p, \rho, C_1, \ldots C_{N-1}) \tag{5}$$

can be determined from the chemical reactions occuring in the flow.

The specific enthalpy is given by

$$h = h(p, \rho, C_1, \ldots C_{N-1}) \tag{6}$$

Using equation (6) to eliminate enthalpy from (3) and substituting from (4),

$$\frac{Dp}{Dt} - a^2 \frac{D\rho}{Dt} + \sum_{i=1}^{N} g_i \frac{(\frac{\partial h}{dC_i})_{p, \rho, C_{j\neq i}}}{(\frac{\partial h}{\partial p})_{\rho, C_j} - \frac{1}{\rho}} = \frac{q + uw}{[(\frac{\partial h}{\partial p})_{\rho, C_j} - \frac{1}{\rho}]} \tag{7}$$

where a is the frozen speed of sound and it is given by

$$a^2 = - \frac{(\frac{\partial h}{\partial \rho})_{p, C_j}}{[(\frac{\partial h}{\partial p})_{\rho, C_j} - \frac{1}{\rho}]} . \tag{8}$$

The specific entropy

$$s = s(p, \rho, C_1, \ldots C_{N-1})$$

can be introduced into equation (7) to obtain

$$(\frac{\partial p}{\partial s})_{\rho, C_j} \frac{Ds}{Dt} = - \sum_{i=1}^{N} g_i [(\frac{\partial p}{\partial C_i})_{\rho, s, C_{j\neq i}} + \frac{(\frac{\partial h}{\partial C_i})_{p, \rho, C_{j\neq i}}}{(\frac{\partial h}{\partial p})_{\rho, C_j} - \frac{1}{\rho}}]$$

$$+ \frac{q + uw}{(\frac{\partial h}{\partial p})_{\rho, C_j} - \frac{1}{\rho}} \tag{9}$$

where another expression for the frozen speed of sound

$$a^2 = \left(\frac{\partial p}{\partial \rho}\right)_{s,\, C_j} \tag{10}$$

has been used.

The gas mixture is assumed to be thermally perfect

$$p = R\rho T \tag{11}$$

where $$R = \sum_{i=1}^{N} C_i R_i \tag{12}$$

and $R_i$ is the specific gas constant of the i-th species.

Assuming the gas mixture to be calorically perfect,

$$h = C_p(T - T_R) + \Sigma C_i h_{f_i} \tag{13}$$

where $C_p$ is the specific heat at constant pressure for the gas mixture, $T$ is the temperature, $T_R$ is the reference temperature for the definition of enthalpy and entropy, and $h_{f_i}$ is the enthalpy of formation of the i-th species

$$C_p = \sum_{i=1}^{N} C_i C_{p_i} \tag{14}$$

The specific heat at constant volume for the gas mixture

$$C_v = \sum_{i=1}^{N} C_i C_{v_i} \tag{15}$$

and the ratio of specific heats

$$\gamma = C_p/C_v \tag{16}$$

There are two possible ways to define the enthalpy of the mixture. If one is going to use the enthalpy of combustion to calculate combustion heat release then the last term in equation (13) is unnecessary. But if one defines $h$ as in equation (13) then the combustion heat release is taken care of with the enthalpy of formation. The specific entropy of the mixture is

$$s = C_p \ln T/T_R - R \ln P/P_R + \ln \prod_{i=1}^{N} f_i^{-C_i R_i} + \sum_{i=1}^{N} C_i s_{f_i} \tag{17}$$

where $P_R$ is the reference pressure for definition of change in entropy, $f_i$ is the mole fraction of the i-th species and $s_{f_i}$ is the entropy of

formation of the i-th species.

The relationship $p = p(\rho, s)$ called the entropic equation of state is

$$p = \frac{(\rho R T_R)^{\gamma}}{P_R^{R/C_v}} \exp\left[\frac{s - \sum_{i=1}^{N} C_i s_{f_i}}{C_v}\right] \prod_{i=1}^{N} f_i^{C_i R_i / C_v} \qquad (18)$$

Equations (11), (13) and (18) can be used to derive the expressions for the partial derivatives in equations (7), (8) and (9). Substituting for the partial derivatives and also for the substantial derivative of density from (1) in equation (7),

$$\frac{Dp}{Dt} + a^2 \rho \frac{\partial u}{\partial x} + a^2 \rho u \frac{d \log_e a}{dx} + \sum_{i=1}^{N} g_i \left(\frac{h_i \rho R}{C_v} - \frac{p \gamma R_i}{R}\right) = (q + uw)\frac{\rho R}{C_v} \qquad (19)$$

where $h_i = C_{p_i}(T - T_R) + h_{f_i}$. (20)

Substituting for the partial derivatives in equation (9)

$$\frac{Ds}{Dt} = -C_v \sum_{i=1}^{N} g_i \left[\log_e \left(\frac{pT_R R}{P_R}\right)\right]\left(\frac{C_v C_{p_i} - C_p C_{v_i}}{C_v^2}\right) - \frac{s_{f_i}}{C_v} - \frac{C_{v_i}}{C_v^2}\left(s - \sum_{i=1}^{N} C_i s_{f_i}\right)$$

$$+ \frac{R_i}{C_v} \log_e f_i - \frac{C_{v_i}}{C_v} \log_e \prod_{i=1}^{N} f_i^{\frac{C_i R_i}{C_v}} + \frac{\rho R h_i}{p C_v} \qquad (21)$$

Choosing a characteristic length $\ell_o$, the velocity of sound $a_o$, pressure $p_o$, and specific gas constant of the ambient air $R_o$, as reference parameters, the non-dimensional forms of equations (19), (2), (21) and (4), respectively, are

$$\frac{\partial P'}{\partial Z} + U \frac{\partial P'}{\partial X} + \gamma_o D A^2 \frac{\partial U}{\partial X} = -\gamma_o D A^2 P + E - B \qquad (22)$$

$$\frac{1}{\gamma_o D}\frac{\partial P'}{\partial X} + \frac{\partial U}{\partial Z} + U \frac{\partial U}{\partial X} = -W \qquad (23)$$

$$\frac{DS}{DZ} = H + Y \qquad (24)$$

$$\frac{DC_i}{DZ} = G_i \qquad (25)$$

$(i = 1, 2, \ldots N-1)$ where

$P' = p/p_o$, $Z = ta_o/\ell_o$, $U = u/a_o$, $X = x/\ell_o$, $D = \rho R_o T_o/p_o$,

$A = a/a_o$, $W = wi_o/a_o^2$, $S = s/R_o$, $G_i = g_i \ell_o/a_o$

$$B = -\sum_{i=1}^{N} G_i \left\{ \frac{DR'}{C_v'} \left[ C_{p_i}' (T' - T_R') + h_{f_i}' \right] - \frac{P' \gamma R_i'}{R'} \right\}$$

$$E = \frac{\gamma_o (Q' + UW) DR'}{C_v'}$$

$$F = U \frac{d \log_e a}{dX}$$

$$H = -C_v' \sum_{i=1}^{N} G_i \left\{ \left[ \log_e \left( \frac{DT_R' R'}{P_R'} \right) \right] \left( \frac{C_{p_i}'}{C_v'} - \gamma \frac{C_{v_i}'}{C_v'} \right) - \frac{S_{f_i}}{C_v'} - \frac{C_{v_i}'}{C_v'^2} \left( S - \sum_{i=1}^{N} C_i S_{f_i} \right) \right.$$

$$\left. + \frac{R_i'}{C_v'} \log_e f_i - \frac{C_{v_i}'}{C_v'} \log_e \prod_{i=1}^{N} f_i^{C_i' R_i' / C_v'} + \frac{DR' h_i'}{P' C_v'} \right\}$$

$$Y = \frac{\gamma_o R' D}{P'} (Q' + UW)$$

and $Q' = {}^{Qt_o}/_{a_o^3}$, $R' = {}^{R}/_{R_o}$, $C_v' = {}^{C_v}/_{R_o}$,

$C_{p_i}' = {}^{C_{P_i}}/_{R_o}$, $T' = {}^{T}/_{T_o}$, $T_R' = {}^{T_R}/_{T_o}$,

$h_{f_i}' = {}^{h_{f_i}}/_{(R_o T_o)}$, $R_i' = {}^{R_i}/_{R_o}$, $S_{f_i} = {}^{S_{f_i}}/_{R_o}$

$h_i' = {}^{h_i}/_{(R_o T_o)}$.

$\gamma_o$ is the ratio of specific heats for the ambient air

## 3. NUMERICAL METHOD

Equations (22) - (25) constitute a set of quasi-linear hyperbolic partial differential equations which can be solved using the method of characteristics. A numerical scheme, the Hartree's hybrid scheme which was used by some earlier workers [3, 4] is also used in this work. In this method, a rectangular grid is imposed on the integration domain and the equations are integrated along the characteristic directions. The dependent variables used are $P'$, $U$, $S$, $C_1$, $C_2$, . . . , $C_{N-1}$.

Following the procedure given by Courant and Hilbert [5] the characteristic curves of equations (22) - (25) can be shown to be

$$\frac{dX}{dZ} = U + A \tag{26}$$

$$\frac{dX}{dZ} = U - A \tag{27}$$

$$\frac{dX}{dZ} = U . \tag{28}$$

Equations (26) and (27) give the downstream and upstream propagation directions in the X - Z plane, of a pressure wave travelling at the frozen speed of sound relative to the fluid. Equation (28) represents N (the number of species) coincident characteristics which is the particle path line.

The compatibility equations along the characteristics of equations (26) and (27), respectively, are

$$\frac{1}{\gamma_o DA}\frac{\delta_+ P'}{\delta Z} + \frac{\delta_+ U}{\delta Z} + AF + W + \frac{B-E}{\gamma_o DA} = 0 \tag{29}$$

and

$$-\frac{1}{\gamma_o DA}\frac{\delta_- P'}{\delta Z} + \frac{\delta_- U}{\delta Z} - AF + W + \frac{E-B}{\gamma_o DA} = 0 \tag{30}$$

where $\frac{\delta_+}{\delta Z}$ is the differentiation following a characteristic having reciprocal slope (U+A) while $\frac{\delta_-}{\delta Z}$ is the differentiation following a characteristic having reciprocal slope (U-A).

The compatibility equations along the characteristic of equation (28) are identically the same as equations (24) and (25).

The characteristics reaching a grid point for different flow velocities are shown in figure 1. The characteristics having slopes (U+A), (U-A) and U are labelled OV, TV and HV respectively. The

finite difference approximation of the compatibility equations are

$$U_V - U_0 + \frac{1}{\gamma_o}\left(\frac{1}{DA}\right)_{OV}(P_V' - P_0') = -(AF + W + \frac{B-E}{\gamma_o DA})_{OV}\Delta Z \qquad (31)$$

$$U_V - U_T - \frac{1}{\gamma_o}\left(\frac{1}{DA}\right)_{TV}(P_V' - P_T') = -(-AF + W + \frac{E-B}{\gamma_o DA})_{TV}\Delta Z \qquad (32)$$

$$S_V = S_H + (H + Y)_{HV}\Delta Z \qquad (33)$$

$$C_{i_V} = C_{i_H} + G_{i_{HV}}\Delta Z \qquad (34)$$

$$(i = 1,2, \ldots, N-1).$$

For the N-th species,

$$C_N = 1 - \sum_{i=1}^{N-1} C_{i_V} \qquad (35)$$

The double subscripts on a term indicates that the term is taken to be the mean of its value at the end points indicated by the two subscripts (see Fig.1).

## 4. BOUNDARY CONDITIONS

The characteristics reaching the right boundary which communicates with the ambient are shown in Fig.2. The flow at the boundary is assumed to be quasi-steady.

### 4.1 Inflow

The inflow is assumed to be isentropic

$$S_V = S_A \qquad (36)$$

where subscript V denotes value at grid point V and A denotes value of the parameter at ambient condition.

The mass fractions of the species are the same as those of the species in the ambient air

$$C_{i_V} = C_{i_A} \qquad (37)$$

$$(i = 1, \ldots N-1).$$

For quasi-steady inflow, the energy equation can be expressed as

$$C'_{p_A} T'_A = C'_p P'^{(\gamma-1)/\gamma}_V T'_R P'^{(1-\gamma)/\gamma}_R \exp\left(\frac{S - \sum_{i=1}^{N} C_i S_{f_i}}{C'_p}\right)\left(\prod_{i=1}^{N} f_i^{C_i R'_i / C'_v}\right)^{1/\gamma} + \frac{\gamma_o}{2} U'^2_V \qquad (38)$$

Equations (29) and (38) were solved to obtain $P'$ and $U$ by Newton's method in 2-dimension [6].

## 4.2 Sonic Inflow

The velocity at the grid point equals the sonic velocity

$$U_V = A_V \qquad (39)$$

But

$$A^2 = \frac{\gamma}{\gamma_o} R' T' \qquad (40)$$

and

$$T' = P'^{(1-\frac{1}{\gamma})} T'^{(\frac{1}{\gamma}-1)}_R P'^{(1-\gamma)/\gamma}_R \exp\left(\frac{S - \sum_{i=1}^{N} C_i S_{f_i}}{C'_p}\right)\left(\prod_{i=1}^{N} f_i^{C_i R'_i / C'_v}\right)^{1/\gamma} \qquad (41)$$

Substituting from (39) - (41) in equation (38),

$$P'_V = \left[\frac{C'_{p_A} T'_A}{C'_p + \gamma R'/2\left(\prod_{i=1}^{N} f_i^{C_i R'_i / C'_v}\right)^{1/\gamma} \exp\left(\frac{S - \sum_{i=1}^{N} C_i S_{f_i}}{C'_p}\right) T'^{(1-\gamma)/\gamma}_R P'^{(1-\gamma)/\gamma}_R}\right]^{\gamma/(\gamma-1)} \qquad (42)$$

Supersonic inflow case is not considered since such a flow velocity is not attainable at an inlet plane in quasi-steady inflow unless a flow which is already supersonic is supplied to the intake.

## 4.3 Subsonic Outflow

For quasi-steady outflow, the static pressure at the exit plane equals the ambient pressure

$$P'_V = P'_A \qquad (43)$$

This equation and the compatibility relations along OV and HV are solved to obtain the values of dependent variables at the boundary.

## 4.4 Sonic/Supersonic Outflow

All the characteristics are washed downstream. Equations (31) -

(35) are solved as for an internal grid point to obtain the values of dependent variables at the boundary.

4.5 Closed End

$$U_V = 0.0 \tag{44}$$

Equation (44) is solved along with the compatibility relations along OV and HV to obtain the values of dependent variables.

4.6 Prescribed Dependent Variables

The values of pressure, temperature, velocity, and mass fractions as functions of time, obtained from experiments, may be prescribed at the boundary.

4.7 Left Boundary

The equations for the left boundary are of the same form as those of the right. The only difference is that the compatibility relation along OV characteristic is replaced with that along TV characteristic.

## 5. COMBUSTION MODEL

Complete oxidation of the fuel is assumed. Thus the products are $CO_2$ and $H_2O$, and it is necessary to take only 5 species into account: $O_2$, $N_2$, fuel vapour and the products.

The following overall reaction equation which was used earlier by Clarke and Craigen [2] is also used in this work

$$\dot{m}_f''' = K\, C_{C_3H_8}^{1.5}\, C_{O_2}^{0.5}\, \rho^2 \exp[-E/R_u T] \tag{45}$$

where $\dot{m}_f'''$ is the mass of fuel consumed per unit volume in a unit time, $K$ is the reaction rate constant, $R_u$ is the universal gas constant, $E$ is the activation energy and subscripts $C_3H_8$ and $O_2$ represent propane and oxygen respectively.

In practice, complete oxidation does not occur and unburned hydrocarbons, CO and $NO_x$ may be found in the exhaust gases. However, the use of overall kinetic approach is inevitable at this stage since with the

present knowledge of chemical kinetics one can not present a reliable detailed kinetic scheme for the reaction of propane with air in unsteady chemically-reacting flow like in pulsed combustor.

By stoichiometry, the species generation rates per unit mass are

$$s_{CO_2} = 2.9941\ \dot{m}_f'''/\rho \tag{46}$$

$$s_{O_2} = -3.628\ \dot{m}_f'''/\rho \tag{47}$$

$$s_{C_3H_8} = -\dot{m}_f'''/\rho \tag{48}$$

$$s_{H_2O} = 1.6341\ \dot{m}_f'''/\rho \tag{49}$$

where subscripts $CO_2$ and $H_2O$ represent carbon-dioxide and water respectively.

An activation energy of $E = 55{,}000$ and a reaction rate constant of $K = 3.0 \times 10^6$ were used in equation (45). These values are within the ranges of literature values of E and K which vary from 21,000 to 168,000 kJ/kmol and from $3.0 \times 10^6 - 4.8 \times 10^8$ $m^3/kg.s$ respectively [2].

## 6. HEAT TRANSFER AND WALL FRICTION

The rate of heat transfer by convection and radiation from the wall to a grid node is

$$Q = h_{C_{in}}\, a_{in}\, (T_w - T_g) + \frac{\epsilon_w + 1}{2}\, \sigma\, \epsilon_g a_{in} (T_w^4 - T_g^4) \tag{50}$$

where $h_{C_{in}}$ is the convective heat transfer coefficient at the inner surface of the duct, $a_{in}$ is the inner lateral surface area of the duct section around the grid, $T_w$ is the wall temperature, $T_g$ is the gas temperature, $\epsilon_w$ is the emissivity of the wall, $\epsilon_g$ is the emissivity of gas and $\sigma$ is the Stefan-Boltzmann constant. The friction factor $C_f$ and the inner surface convective heat transfer coefficient $h_{C_{in}}$ are obtained using equations of the forms relating friction factor and Nusselt number to local flow parameters in steady flow as suggested by

Bannister [7].

$$C_f = 0.25\ Re_d^{-0.25} \tag{51}$$

$$h_{C_{in}}\, d/k = 0.023\ Re_d^{0.8}\ Pr^{0.33} \tag{52}$$

where $d$ is the duct diameter, $k$ is the thermal conductivity of the gas, $Re$ is Reynolds number and $Pr$ is Prandtl number. The frictional force per unit mass on the fluid element at the grid is

$$w = \frac{4C_f}{d}\ u|u|. \tag{53}$$

## 7. APPLICATION TO A SHOCK TUBE

The calculations were carried out on the CDC CYBER 175 computer. To test the model, it was applied to predict the pressure at the left-end of a uniform diameter shock tube which was closed. The shock tube which was initially filled with compressed air at a nondimensional pressure of 2.83 and temperature of 1.346 discharged its content isentropically to the atmosphere through the right end which was fully open. The air was taken as a mixture of 76.7% nitrogen and 23.3% oxygen by mass.

The result of the computation is compared with that obtained by Rudinger [8] using a graphical method of characteristics in Fig.3. Figure 4 shows the results predicted with the model using 41 and 501 grid points.

The time step for a certain grid size was chosen in accordance with the Courant-Friedrichs-Lewy stability criterion [3] which requires that

$$\Delta Z \leq \frac{\Delta X}{A + |U|}. \tag{54}$$

## 8. APPLICATION TO A PULSED COMBUSTOR

The model was applied to predict the operation of a propane-fuelled quarter-wavelength, organ pipe pulsed combustor of the type used by Hanby [9] and Clarke and Craigen [2]. This combustor is closed at the left end except for a little opening through which fuel and air is admi-

ttad. The right end is fully open to the atmosphere. The combustor is of length 1.985 m and diameter 51 mm.

For the computation, pressure-time variation at the left end is assumed to be sinusoidal and the amplitude measured experimentally by Clarke and Craigen [2] are used as data input. The mean gas temperature at the left end (X = 0) is taken to be 600 K. The initial pressure and temperature distribution in the pulsed combustor at time Z = 0 are taken to be atmospheric pressure and 4.5 times the absolute ambient temperature.

Cyclic operation is caused by the effect of the left and right end boundary conditions and the intermittent combustion. Combustion was allowed to take place in any grid having fuel and oxygen while the pressure in that grid is rising from the mean value towards the maximum according to Rayleigh's criterion [10]. The frequency of the cyclic operation of the pulsed combustor was taken to be 90 Hz. The computation converged to cyclic operation before the 12th cycle.

Figure 5 shows the comparison of the computed pressure amplitudes in the combustor with the experimental results of Clarke and Craigen [2] for a fuel flow rate of 0.56 kg/h and air/fuel ratio of 18.9. The pressure amplitude and mean temperature distribution in the combustor for the case when the mass flow rate of the fuel is 0.93kg/h and the air/fuel ratio is 16.0 are shown in Figure 6.

Heat transfer from the external surface of the pipe to the ambient air is by natural convection and radiation. Natural convection heat transfer coefficient $h_{C_{ex}}$ is calculated from the empirical relation for free convection from horizontal pipe [11].

$$h_{C_{ex}} d/k = 0.53(Gr\ Pr)^{0.25} \qquad (55)$$

where $h_{C_{ex}}$ is the convective heat transfer coefficient at the external surface of the duct and Gr is Grashoff number.

The time-mean temperature of the wall element around each grid node was calculated using

$$\sum_{i=1}^{N_s} \{[h_{C_{in_i}} (T_{t_i} - T_w) + \frac{(\epsilon_w + 1)}{2} \sigma \epsilon_g (T_i^4 - T_w^4)] a_{in} (\Delta t)_i\}$$
$$- [\sigma \epsilon_w (T_w^4 - T_A^4) + h_{C_{ex}} (T_w - T_A)] a_{ex} \sum_{i=1}^{N_s} (\Delta t)_i \qquad (56)$$

where $(\Delta t)_i$ is time interval of the i-th step,

$T_{t_i}$ is the stagnation temperature in the i-th step

$N_s$ is number of time steps in the cyclic period.

Newton-Raphson method was used to solve for $T_w$ in equation (56). The gas emissivity $\epsilon_g$ used in the computation was 0.04 which is one quarter of the value used by Clarke and Craigen [2].

## 9. DISCUSSION OF RESULTS

The agreement between the result predicted with the model and the results of the graphical methods in Fig.3, is quite good when one remembers that the numerical method involves a lot of interpolations. The results in Fig.4 illustrate the well known advantage of numerical method of characteristics that reasonable results can be obtained even with coarse grid size.

In figure 5, there is only a qualitative agreement between results predicted with the model and the experimental result. Only such agreement can be expected in this work because of the assumptions made in the data input. The assumed sinusoidal pressure-time variation at the left end and the constant gas temperature there are not accurate. Also the assumed constant mass flow rate at the left end is much simpler than the actual mass flow rate which varies with pressure at the left end. These crude data input had to be used in the absence of better values.

The peaking of the mean gas temperature at a distance of about X = 0.1 agrees well with the experimental result of Clarke and Craigen [2]. It should be noted that the value of the mean gas temperature of 1.01 at the right end is not the average efflux gas temperature. The mean gas temperature towards the right end is that low because of the reverse flow from the ambient that occurs during part of the cycle in addition to the fact that an appreciable percentage of the combustion heat release is lost through the wall to the ambient. Such a low temperature towards the right end of the combustor was observed by Clarke and Craigen [2].

## 10. CONCLUSION

An algorithm for computing one-space dimensional unsteady chemically reacting flow has been presented. Its validity has been proved by results obtained from its applications to a shock tube and a pulsed combustor.

To obtain reasonable gas temperature in a chemically reacting flow such as occurs in a pulsed combustor, without resorting to using excessively high gas emissivity, one needs to consider the effect of chemical reaction on the gas composition.

## ACKNOWLEDGEMENT

The provision of computer time for this work on Control Data Cyber-175 computer by the University of Calgary, Canada, is gratefully acknowledged.

## REFERENCES


[1] Cline, M.C., "The Analysis of Nonequilibrium, Chemically Reacting, Supersonic Flow in Three Dimensions", Ph.D. Thesis, Purdue University, 1971.

[2] Clarke, P.H., Craigen, J.G., "Mathematical Model of a Pulsating Combustor", Paper C54/76, Sixth Thermodynamics and Fluid Mechanics Convention, I. Mech. E. Conference Publications 1976-6, pp.221-228.

[3] Benson, R.S., Garg, R.D., and Woollatt, D., "A Numerical Solution of Unsteady Flow Problems", Int. J. Mech. Sci., vol.6, 1964, pp.117-144.

[4] Issa, R.I., and Spalding, D.B., "Unsteady One-dimensional Compressible Frictional Flow with Heat Transfer", Journal of Mech. Eng. Sci., Vol.14, No.6, 1972, pp.365-369.

[5] Courant, R., and Hilbert, D., Method of Mathematical Physics, Vol.II, Interscience Publishers, John Wiley and Sons, New York, 1962.

[6] Acton, F.S., Numerical Methods that work, Harper and Row Publishers, New York, 1970.

[7] Bannister, F.K., "Influence of Pipe Friction and Heat Transfer on Pressure Waves in Gases: Effects in a Shock Tube", Journal of Mech. Eng. Sci., vol.6, No.3, 1964, pp.278-292.

[8] Rudinger, G., Nonsteady Duct flow Wave-Diagram Analysis, Dover Publications Inc., New York, 1969.

[9] Hanby, V.I., "Convective Heat Transfer in a Gas-Fired Pulsating Combustor", ASME paper No.68-WA/FU-1, Dec. 1968.

[10] Putnam, A.A., Combustion-Driven Oscillations in Industry, Elsevier, New York, 1971.

[11] Holman, J.P., Heat Transfer, McGraw-Hill Book Co., New York, 1981.

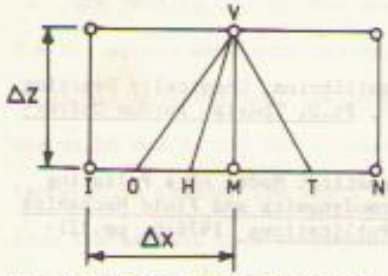


(a) Subsonic Flow to the Right.

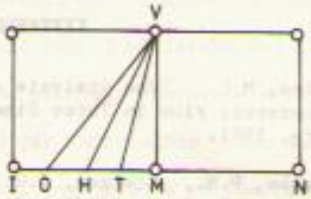


(b) Supersonic Flow to the Right.

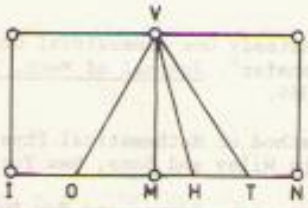


(c) Subsonic Flow to the left.

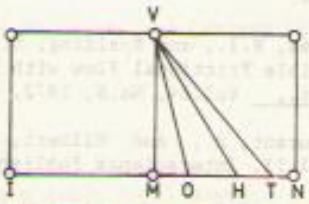


(d) Supersonic Flow to the Left.

FIGURE 1: THE CHARACTERISTICS REACHING AN INTERNAL GRID POINT

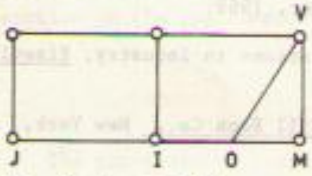


(a) Subsonic Inflow.

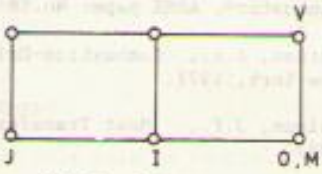


(b) Sonic Inflow.

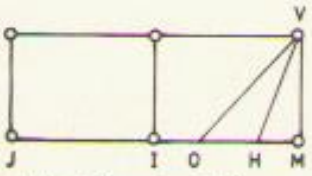


(c) Subsonic Outflow.

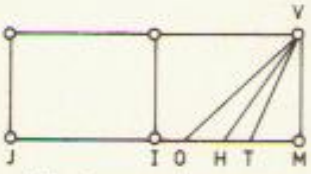


(d) Supersonic Outflow.

**FIGURE 2: THE CHARACTERISTCS REACHING THE RIGHT BOUNDARY GRID POINT.**

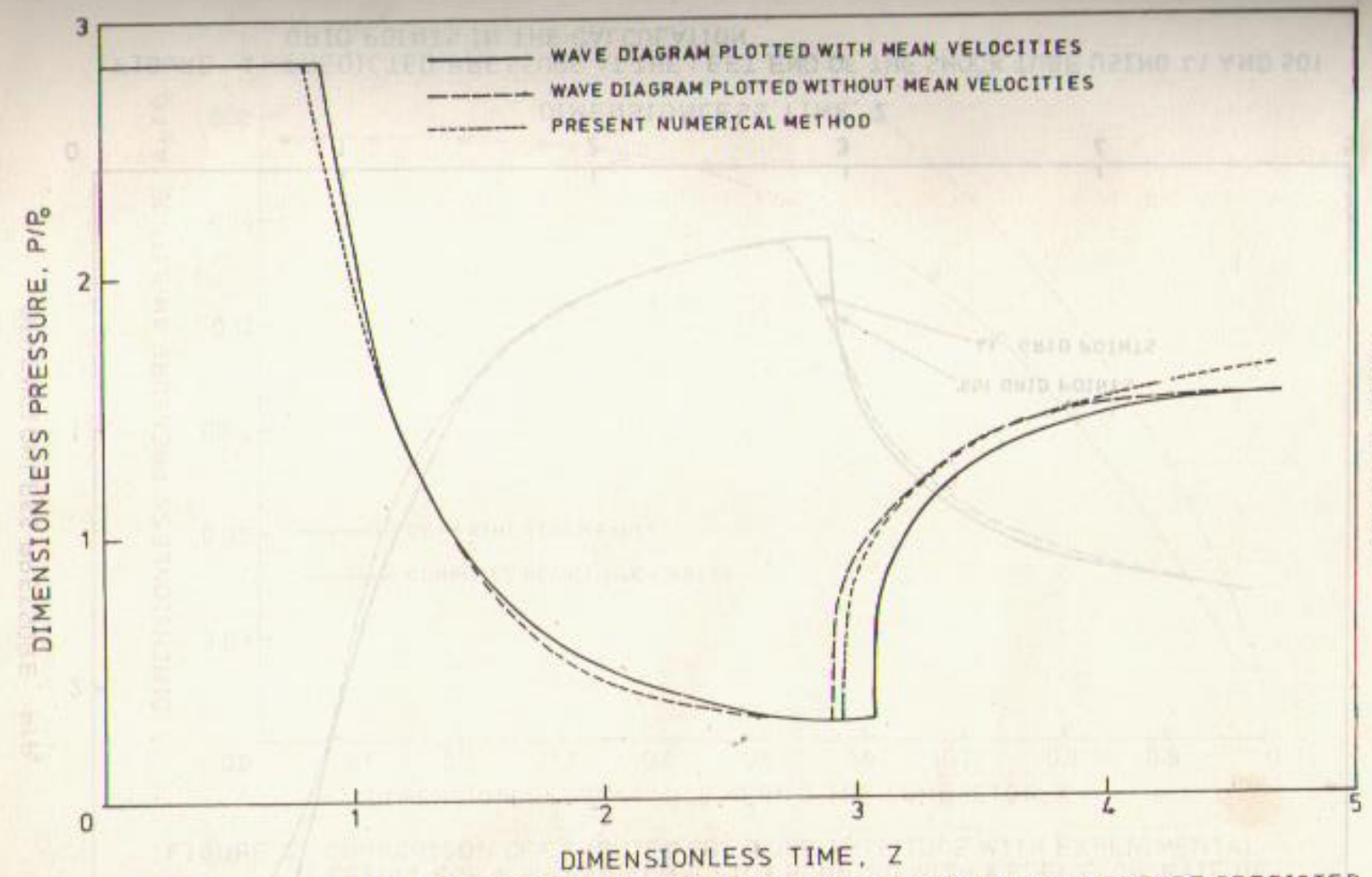


FIGURE 3 : COMPARISON OF PRESSURE AT THE CLOSED LEFT END OF A SHOCK TUBE PREDICTED WITH THE MODEL WITH THE RESULTS OBTANED BY RUDINGER USING A GRAPHICAL METHOD OF CHARACTERISTICS.

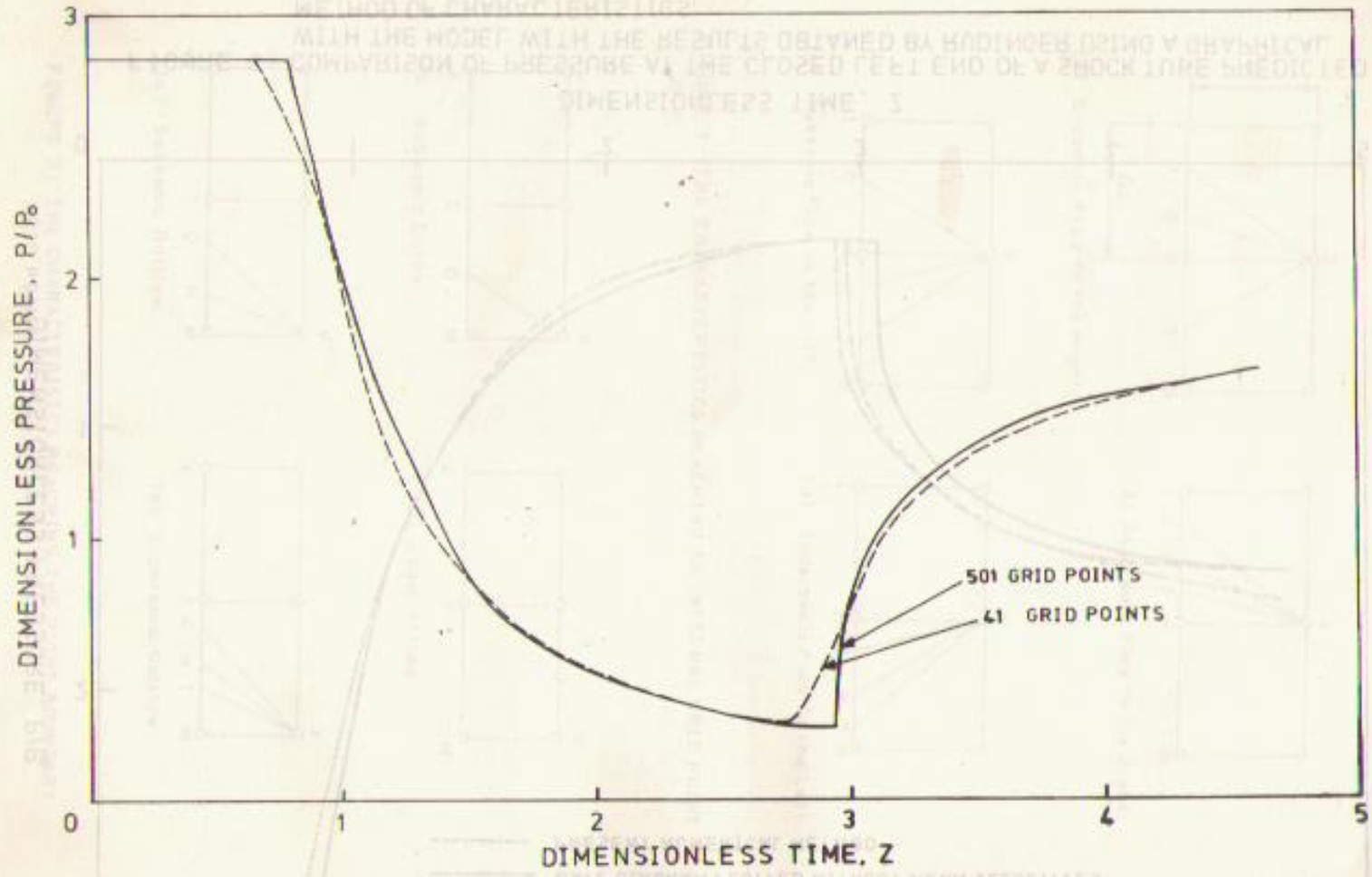


FIGURE 4: PREDICTED PRESSURE AT THE LEFT END OF THE SHOCK TUBE USING 41 AND 501 GRID POINTS IN THE CALCULATION

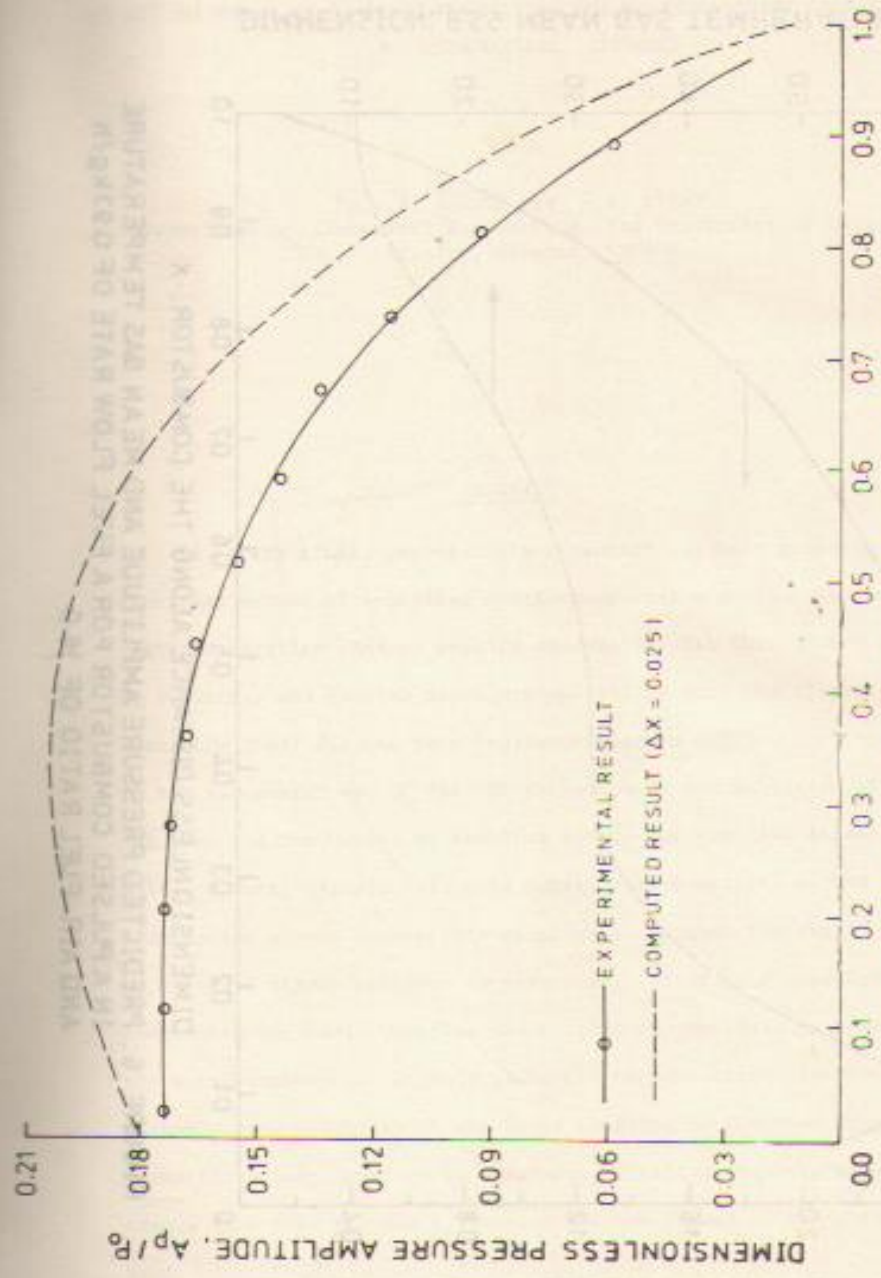


FIGURE 5 - COMPARISON OF COMPUTED PRESSURE AMPLITUDE WITH EXPERIMENTAL RESULT FOR A PULSED COMBUSTOR RUNNING WITH A FUEL FLOW RATE OF 0.56kg/h AND AIR-FUEL RATIO OF 18.9.

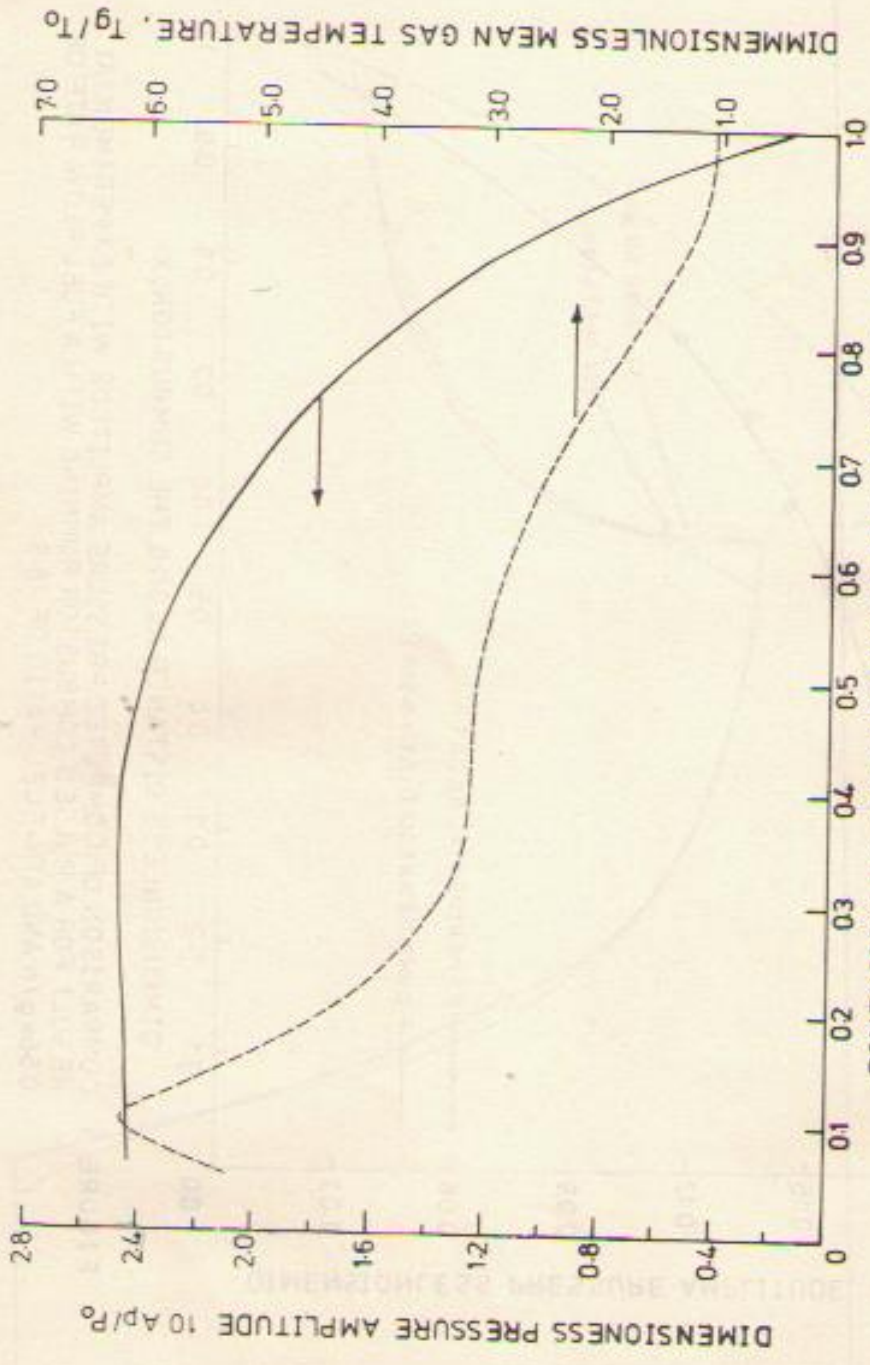


**FIGURE 6: PREDICTED PRESSURE AMPLITUDE AND MEAN GAS TEMPERATURE IN A PULSED COMBUSTOR FOR A FUEL FLOW RATE OF 0.93kg/h AND AIR-FUEL RATIO OF 16.0.**